Cement and Concrete Research 137 (2020) 106213

Contents lists available at ScienceDirect

Cement and Concrete Research

journal homepage: www.elsevier.com/locate/cemconres

Formation of shlykovite and ASR-P1 in concrete under accelerated alkali-silica reaction at 60 and 80 °C

Zhenguo Shi[a,*], Solmoi Park[b,c], Barbara Lothenbach[a,d], Andreas Leemann[a]

[a] Laboratory for Concrete & Construction Chemistry, Swiss Federal Laboratories for Materials Science and Technology (Empa), 8600 Dübendorf, Switzerland
[b] Department of Civil Engineering, Pukyong National University, 48513 Busan, Republic of Korea
[c] Department of Civil and Environmental Engineering, Korea Advanced Institute of Science and Technology (KAIST), 34141 Daejeon, Republic of Korea
[d] Department of Structural Engineering, Norwegian University of Science and Technology (NTNU), 7491 Trondheim, Norway

ARTICLE INFO

Keywords:
Alkali-silica reaction
Shlykovite
Concrete
Aggregate
Temperature

ABSTRACT

Three types of alkali-silica reaction (ASR) products, i.e., crystalline K-shlykovite, Na-shlykovite and nano-crystalline ASR-P1, have recently been synthesized at 80 °C. It is critical to verify the formation of these ASR products in concrete in order to transfer the knowledge of ASR gained from the synthesized products to the ones formed in field concrete. Therefore, ASR products formed in concrete exposed to KOH, NaOH or mixture of KOH/NaOH solution at 60 and 80 °C are analyzed using Raman spectroscopy and scanning electron microscopy with energy-dispersive X-ray spectroscopy. The results show that at temperature between 60 and 80 °C K-shlykovite and ASR-P1 are formed in concrete exposed to KOH or a mixture of KOH/NaOH solution, whereas Na-shlykovite is formed in concrete exposed to NaOH solution. Moreover, K-shlykovite and Na-shlykovite do not co-precipitate in the same concrete, not even in the concrete exposed to the mixture of KOH/NaOH solution.

1. Introduction

Alkali-silica reaction (ASR) has caused damage to concrete structures worldwide including bridges, dams and pavements [1–3]. Despite significant research progress over the past 80 years as reviewed in [4–6], our knowledge on ASR such as the molecular structure of the ASR products, the precise formation conditions of ASR and the expansion mechanisms, are only recently advanced [7–13]. On one hand, this is due to the slow kinetics of ASR in field concrete that usually takes years or up to decades for cracks to form, making it difficult to be diagnosed. On the other hand, only small amounts of ASR products are formed in veins of concrete aggregates. Their volume is in the micrometer-scale, which makes it impossible to be characterized with conventional laboratory techniques such as solid-state ^{29}Si magic-angle spinning nuclear magnetic resonance (^{29}Si MAS NMR), thermogravimetric analysis (TGA) or X-ray diffraction analysis (XRD).

Due to the slow kinetics of ASR in field concrete, accelerated testing methods involving elevated temperatures, e.g. 38, 60, 80 and 150 °C [14,15], were employed in laboratory tests and studies of ASR. Several studies attempted to establish a link between expansion obtained in accelerated tests and field exposed concrete [16–19]. Going one step further, the expansion, the type of aggregates reacting and the composition of the ASR products formed have been analyzed in the concrete prism test and concrete structures [20]. Still, the debate about the representativeness of the tested ASR performance at elevated temperature is ongoing. On one hand, this is caused by some discrepancies between the behavior of laboratory tested and field exposed concrete. On the other hand, a more in-depth knowledge about the ASR products is needed to bridge the gap between accelerated tests and field ASR.

In addition to the elevation of the reaction temperature, additional amount of alkalis are also introduced to accelerate ASR by either boosting alkalis of cement or exposing samples to alkaline solution or a combination of both [21–23]. Although in most cases Portland cement contains more K than Na, NaOH is often used to prepare the exposure solution for accelerated tests at 80 °C [24,25]. NaOH is chosen because the total alkali content of Portland cement is usually expressed as Na_2O-equivalent (wt% Na_2O_{eq} = wt% Na_2O + 0.658 × wt% K_2O). Clearly, such an approach is highly empirical as it ignores the influence of alkali types on ASR. Only a limited number of studies have reported that concrete boosted with different types of alkalis show significantly varying expansion, indicating that it is necessary to consider the types of alkalis when testing the ASR performance of concrete [26].

Recent research based on synthetic samples and comparison with few concrete samples have demonstrated that temperature affects the types of crystalline ASR products formed [9,27]. All of them have layer-silicate-sheet structures and similar chemical compositions but different

* Corresponding author.
E-mail address: zhenguo.shi@empa.ch (Z. Shi).

https://doi.org/10.1016/j.cemconres.2020.106213
Received 31 March 2020; Received in revised form 17 July 2020; Accepted 25 August 2020

d-spacings for the diffractions with lowest 2θ values: 12.0 Å (< 40 °C), 10.8 Å (around 40 °C), and 13.1 Å (80 °C for K- and Na-shlykovite: $KCaSi_4O_8(OH)_3{\cdot}2H_2O$ and $NaCaSi_4O_8(OH)_3{\cdot}2.3H_2O$). The K-shlykovite and Na-shlykovite were named after the mineral shlykovite ($KCa[Si_4O_9(OH)]{\cdot}3H_2O$) first reported in [28], since they have similar layer-silicate structure with its SiO_4^{4-} tetrahedron charge-balanced by K^+ (or Na^+) and Ca^{2+} in the main layer and by H^+ in the interlayer [9]. In addition, a nano-crystalline ASR-P1 ($K_{0.52}Ca_{1.16}Si_4O_8(OH)_{2.84}{\cdot}1.5H_2O$) was also observed in a sample synthesized at 80 °C, which also has a layered-silicate structure according to its ^{29}Si MAS NMR data [9]. The results also showed that the ASR products formed at 80 °C depend on the types of alkali sources: K-shlykovite and ASR-P1 were formed in the K-rich samples, whereas Na-shlykovite ($NaCaSi_4O_8(OH)_3{\cdot}2.3H_2O$) was formed when Na was used as the only alkali source [9]. It is expected that formation of different types of ASR products may contribute to the observed differences in the expansion of concrete boosted with different types of alkalis. Successful syntheses of the ASR products have allowed their characterizations with various types of aforementioned laboratory techniques [9–11,27]. The obtained results significantly advanced our understanding about ASR with respect to the structure of the ASR products, ASR formation conditions predicted by thermodynamic modelling and influence of temperature on the mineralogy of the ASR products. Therefore, there are urgent needs to transfer such knowledge from the synthesized products to the ones formed in field concrete. To reach this goal, the formation of the same ASR products in concrete as in synthetic samples first needs to be verified. Micro-Raman and XRD data from recent studies have indicated that K-shlykovite resembled the crystalline ASR product identified in the ASR concrete prism test at 60 °C [9,27,29]. In few cases, K-shlykovite is also observed in field concrete as the surface temperature of concrete at some exposure sites can reach a value of 60 °C due to solar radiation [30]. Formation of ASR-P1 was also observed in concrete samples exposed to KOH solution at 80 °C based on Raman spectra [31]. Such a comparison has not yet been made for Na-shlykovite, since data is available for Na-rich ASR products in concrete samples.

In a parallel study, ASR products formed in concrete at 38 and 60 °C have been analyzed [32]. The crystalline product synthesized at 40 °C was found be similar to that formed in the concrete prism test at 38 °C [27,32]. However, the parallel study mainly focused on K-rich samples as sole Na_2O-boosting/exposure is not commonly applied for these two temperature conditions. In the current study, ASR products formed at 60 and 80 °C are analyzed. In order to identify all types of ASR products formed at these temperatures, namely K-shlykovite, ASR-P1 and Na-shlykovite, the prepared concrete prisms are exposed to sole KOH, NaOH and mixture of KOH/NaOH solutions. The ASR products are analyzed with micro-Raman spectroscopy and scanning electron microscopy with energy-dispersive X-ray spectroscopy (SEM/EDS).

2. Experimental procedure

2.1. Materials and samples

Concrete prisms (40 × 40 × 160 mm^3) were produced with 500 kg/m^3 Portland cement (CEM I 42.5, see Table 1) and a water/cement ratio of 0.50. Aggregates from Uri Switzerland were used (1537.3 kg/m^3) in three different grain size fractions (2/4 mm: 40 wt%; 4/8 mm: 25 wt%; and 8/11.5 mm: 35 wt%; see Table 2). The prisms were demolded after 24 h, followed by immersion in 0.4 mol/L solutions of KOH, NaOH and mixture of KOH/NaOH (with molar ratio of 3/1) at 60 and 80 °C. Four prisms were placed in each container (4 L), three for length and mass change measurements and one reserved for SEM/EDS analysis and Raman spectroscopy. The samples used for SEM/EDS analysis were cut to an appropriate size and dried in an oven for three days at 50 °C, followed by epoxy impregnation, polishing and carbon-coating. For this type of samples, the back-scattering electron (BSE) mode was used. The samples for SEM imaging in the secondary-electron mode (SE) and Raman spectra collection were obtained from cut concrete sections by splitting reacted aggregate along veins filled with ASR products using a chisel and hammer. In addition, the ASR products precipitated in air voids adjacent to aggregates split that way were also analyzed.

Table 2
The mix design of concrete used for ASR concrete prism test.

Materials	Proportions (kg/m^3)
Cement	500
Water	250
Sand (2/4)	615
Coarse aggregate (4/8)	384
Coarse aggregate (8/11.5)	538

2.2. Analytical methods

The length and mass of the concrete prisms were regularly measured up to 8 weeks and 20 weeks for the concrete stored at 60 and 80 °C, respectively. One additional measurement was conducted after 23 weeks for concrete stored at 80 °C. The mass change (g/cm^3) is reported in gram per volume of the prisms. At the end of length measurements after 20 and 23 weeks, Raman spectra and SEM images were acquired from aggregates with crack width > 10 μm.

Micro-Raman spectroscopy was conducted using the Bruker Senterra instrument equipped with a Peltier-cooled CCD detector and operated with the software Opus 6.5. The wave-length of the used laser was 532 nm. The measurements were operated at 20 mW. The length magnification was 50×. The spectral acquisition time was 20 s and spectrum resolution in the used frequency range of 110–1560 cm^{-1} was 3–5 cm^{-1}. About 10–20 spectra were collected per sample. The spectra were averaged, background corrected and normalized.

SE images of the ASR products were collected using a scanning electron microscope (SEM) FEI Quanta 650 with a Large Field Detector (LFD) on the fractured surface of the concrete. An acceleration voltage of 10–12 kV and a spot size 3–4 were used for SE-imaging. A FEI Quanta was used at an acceleration voltage of 12 kV and a spot size 4.0 to acquire BSE-images. Chemical analysis was performed by EDS with a Thermo Noran Ultra Dry 60 mm^2 detector and Pathfinder X-Ray Microanalysis Software.

3. Results

3.1. Length and mass change

The changes in the length of concrete prisms exposed to three different alkali solutions (i.e., KOH, NaOH and mixture of KOH/NaOH solutions) at 60 and 80 °C are shown in Fig. 1. The results show that the increase in length is faster at higher temperature within the first 8 weeks. A similar rate of the length change is observed between concrete samples exposed to KOH solution and mixture of KOH/NaOH

Table 1
Chemical composition (mass%) of the cement (CEM I 42.5).

SiO_2	Al_2O_3	Fe_2O_3	Cr_2O_3	MnO	TiO_2	P_2O_5	CaO	MgO	K_2O	Na_2O	SO_3	LOI
20.14	4.56	3.25	0.013	0.05	0.368	0.24	63.0	1.9	0.96	0.16	3.25	2.06

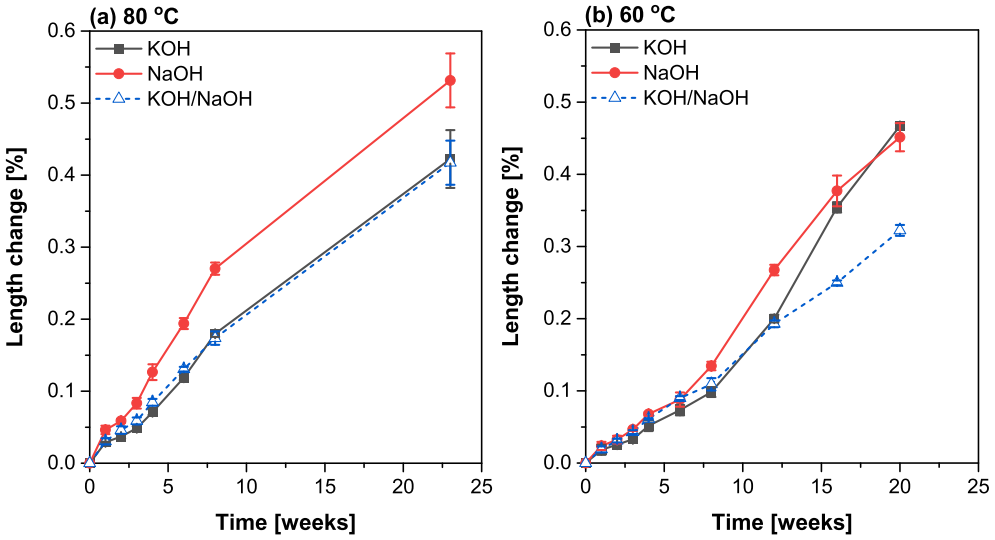

Fig. 1. Length change of the concrete after exposure to alkali solutions at 60 and 80 °C.

solution during the entire period of exposure for concrete stored at 80 °C (Fig. 1a), and during the first 12 weeks for concrete stored at 60 °C (Fig. 1b). Overall, significant increase in length is observed for all samples after storage of about 20 weeks. They show cracks filled with whitish products on the concrete surface.

In addition to the length change, the mass change of the same concrete prisms is also obtained as shown in Fig. 2. A rapid increase in the mass is observed within the first 6 weeks for concrete stored at 80 °C (Fig. 2a), and within the first 12 weeks for concrete stored at 60 °C (Fig. 2b), corresponding to their development of length. Afterwards, the gain in mass is significantly smaller indicating a slowdown of the reaction. A rough correlation between the length change and mass change is shown in Fig. 3. Below the length change of 0.2%, the length increases with the increase of mass, while continuous increase of length is observed despite no further increase of mass at length change over 0.2%. The results indicate a continuous propagation of cracks at the later stage of ASR.

3.2. Characterization of the ASR products

3.2.1. Raman spectra

Raman spectra have recently been obtained for synthesized K-shlykovite, ASR-P1 and Na-shlykovite [9]. The assignments of the corresponding Raman bands are also given in that paper. These data are used as reference to identify the ASR products formed in concrete of the current study. Fig. 4 shows the comparison of the Raman spectra between synthetic ASR products (both crystalline shlykovite and nanocrystalline ASR-P1) and those formed in different concrete samples exposed to sole KOH, NaOH and mixture of KOH/NaOH solutions at 60 and 80 °C. The Raman spectra of the crystalline ASR products formed in concrete exposed to solutions of KOH (Fig. 4a) and mixture of KOH/NaOH (Fig. 4b) at both 60 and 80 °C strongly resemble that of K-shlykovite. In contrast, the Raman spectra of the crystalline ASR products formed in concrete exposed to NaOH solution at both temperatures resemble to that of Na-shlykovite (Fig. 4c). Raman spectra identical to that of Na-shlykovite cannot be found in the concrete exposed to the mixture of KOH/NaOH solution, indicating that K-shlykvoite and Na-shlykovite do not co-exist in the same concrete. For all concrete prisms exposed to the same alkali solution, the same crystalline ASR products are formed in the veins of aggregates, and also in some of the air voids close to aggregates but within cement paste.

In contrast to the crystalline ASR products, formation of the amorphous ASR products in the studied concrete is quite limited and it is more difficult to identify them. The Raman spectra of the few identified

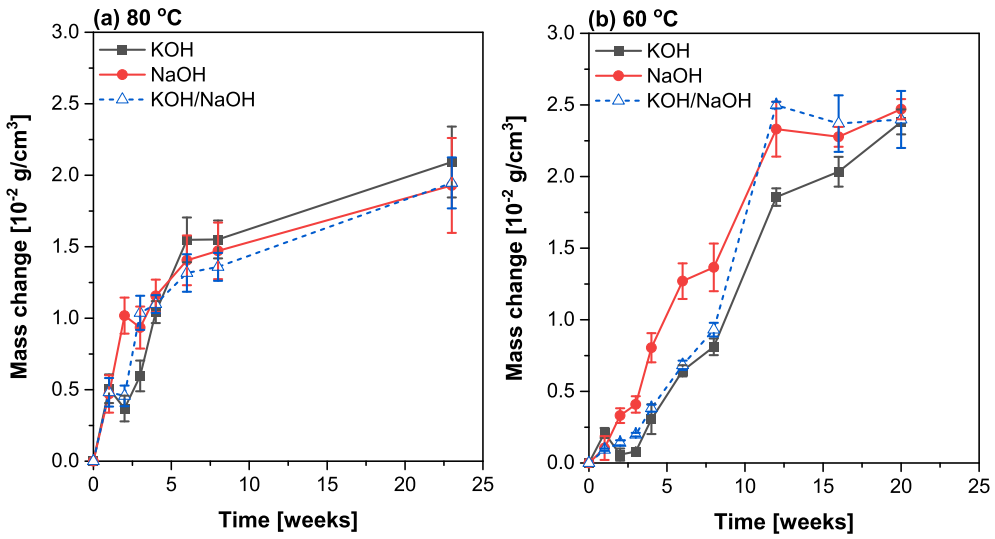

Fig. 2. Mass change of the concrete after exposure to alkali solutions at 60 and 80 °C.

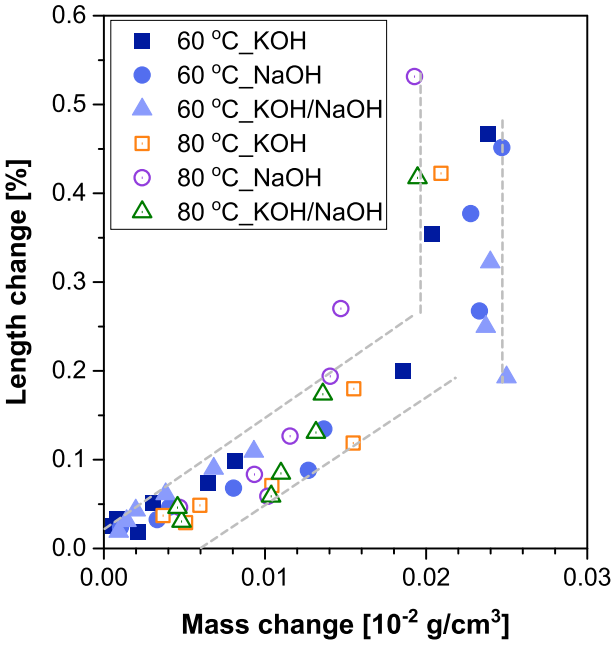

Fig. 3. Relationship between length change and mass change.

spots for the amorphous ASR products are very similar to that of synthetic ASR-P1 as shown in Fig. 4d, although some unknown bands from impurities (e.g. carbonate indicated by * in the figure) are present in the measured spots. Similar to the crystalline ASR products, ASR-P1 is also observed in both veins in aggregates and some air avoids in cement paste adjacent to aggregates. However, their locations are very close to the interfacial transition zone (ITZ) of concrete. A previous study based on a synthetic system showed that ASR-P1 could only form in presence of K [9]. In the present study, ASR-P1 is also by chance observed in concrete exposed to sole NaOH solution, which might be attributed to the high K content in the cement used.

3.2.2. Morphology

The morphologies of the crystalline ASR products formed in aggregates as observed in the split samples are shown in Fig. 5. Similar morphologies of the crystalline ASR products are observed in samples exposed to KOH and mixture of KOH/NaOH solutions at both 60 and 80 °C. All of them have an elongated plate-like morphology. The aspect ratio of the plate varies significantly, approaching a needle-like form in a few cases. This type of morphology is typical for K-shlykovite, as shown in synthetic samples [9]. In contrast to K-shlykovite, Na-shlykovite also shows a plate-like morphology, but more isometric in its dimension [9]. This isometric plate-like feature is observed for the crystalline ASR products formed in the aggregates of concrete exposed to NaOH solutions at both 60 and 80 °C.

Some amorphous ASR products within the cracks of aggregates but close to the ITZ are also observed for example in concrete exposed to the mixture of KOH/NaOH solution at 60 °C as shown in Fig. 6. The Raman spectrum collected on the same location as shown in Fig. 4d indicates that this amorphous ASR product (labeled as KOH/NaOH) is very similar to synthetic ASR-P1. The similarity between ASR-P1 and the amorphous ASR products formed in concrete exposed to sole KOH and mixture of KOH/NaOH solutions is confirmed by comparison of their Raman spectra in Fig. 4d.

3.2.3. Chemical compositions

The chemical compositions of both crystalline and amorphous ASR products were measured on a polished section of concrete samples as shown in Fig. 7. Most of the ASR products are formed within veins present in aggregates, where crystalline ASR products are formed in the interior of aggregates and amorphous ASR products are formed also in aggregates but close to the ITZ. The morphologies of the crystalline ASR products as described in the previous paragraph apply as well for the polished samples as far as it can be assessed in 2D (see Fig. 7a, c and e). In contrast to the crystalline ASR products, identification of the amorphous ASR products is more difficult due to their extremely low amounts. These amorphous ASR products are formed close to the ITZ in much smaller volume (few μm, see Fig. 7b, d and f) compared to the crystalline ones (20–30 μm). Thus, only few locations allow EDS analysis of the amorphous ASR products.

The EDS results of the crystalline and amorphous ASR products are shown in Fig. 8 and with their average atomic ratios summarized in Table 3. The alkali/Si ratios are expressed as K/Si and Na/Si ratio rather than (K + Na)/Si ratio to make distinction between K- and Na-ASR products. For all crystalline ASR products (see Fig. 8a, c and e from one of the selected locations for each sample), the results show an average Ca/Si ratio of 0.17–0.22 with little variations for all concrete samples independent of exposure alkalis and temperatures, whereas significant variations of K/Si ratio or Na/Si ratios from 0.15 to 0.4 are observed for these ASR products. For concrete exposed to both KOH and mixture of KOH/NaOH solutions (see Fig. 8a and e), only traces of Na are identified in the crystalline ASR products in few locations. This observation supports the observation that K-shlykovite is the only crystalline ASR product formed in concrete exposed to KOH and mixture of KOH/NaOH solutions, although a significant amount of Na is present in the concrete exposed to the mixture of KOH/NaOH solution.

Compared to the crystalline ASR products, both Ca/Si ratio and alkali/Si ratios exhibit significant variations in the amorphous ASR products as shown in Fig. 8b, d and f. Moreover, both K and Na are present in this type of products. Overall, higher K/Si ratio than Na/Si is observed for the amorphous ASR products formed in concrete exposed to KOH and mixture of KOH/NaOH solutions, and higher Na/Si ratio in the case of sole NaOH exposure. The Na/Si ratio of the amorphous ASR products is also higher for KOH/NaOH exposed concrete than for the sole KOH exposed concrete.

4. Discussion

4.1. Types and formation of ASR products in concrete

The Raman spectra and SEM/EDS for the crystalline ASR products show consistent results. The Raman spectra show that K-shlykovite is formed in concrete exposed to sole KOH (in Fig. 4a) and mixture of KOH/NaOH (in Fig. 4b) solutions at 60 and 80 °C. Na-shlykovite is only formed in concrete exposed to sole NaOH solution (Fig. 4c). Furthermore, SEM images in Figs. 5 and 7 show an elongated plate-like morphology for K-shlykovite and isometric plate-like forms for Na-shlykovite, similar to the ones reported for the synthetic ASR products [9]. Again these observations are consistent with their chemical compositions, where Na is almost absent in the crystalline ASR products formed in the concrete exposed to KOH (Fig. 8a) and mixture of KOH/NaOH (Fig. 8c) solution, and K is almost absent in that exposed to NaOH solution (Fig. 8b). These results also confirm that K-shlykovite and Na-shlykovite do not co-precipitate within the same concrete, which is also in line with the observation from synthetic systems [9].

Due to the small amounts of amorphous ASR products present in aggregates, it is challenging to analyze identical locations by Raman spectroscopy and SEM/EDS. Moreover, their chemical compositions vary in the same concrete and the morphology does not show distinct features. It is unclear whether the analyzed amorphous ASR product is a single phase containing both K and Na, or they are mixture of K-ASR product and Na-ASR product. Consequently, it is difficult to make a direct link between the Raman spectra in Fig. 4 and the SEM/EDS results in Figs. 7 and 8. Only one spot of the amorphous ASR products is captured which allows the Raman spectra of this amorphous ASR product (labeled as “KOH/NaOH 60 °C_crack” in Fig. 4d) to be linked with

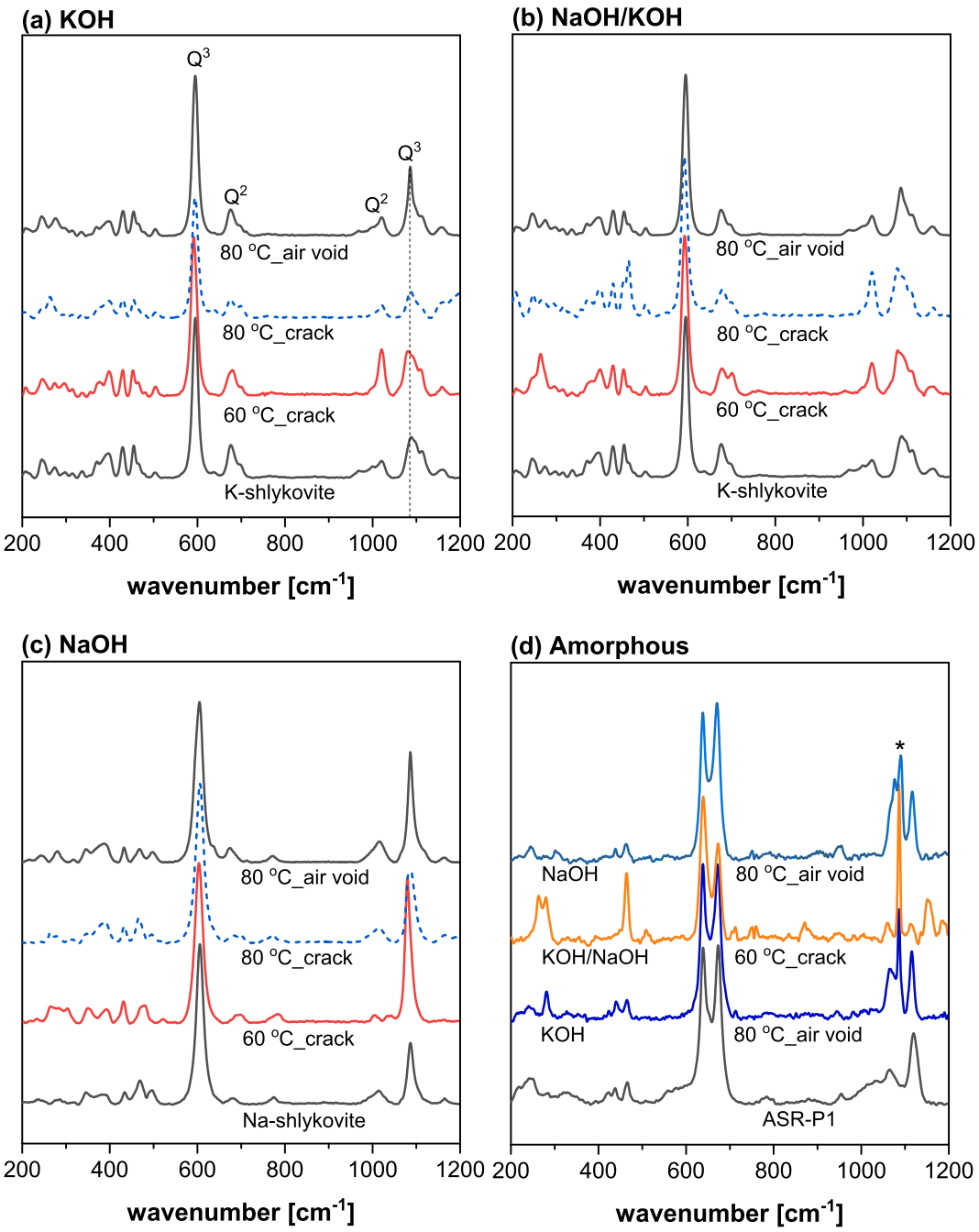

Fig. 4. Comparison of the Raman spectra between synthetic ASR products and those formed in cracks of aggregates and some air voids adjacent to the ITZ of concrete samples. The asterisk (*) indicates an unknown impurity, which is most likely related to calcium carbonate. The Raman spectra of synthetic ASR products (K-shlykovite, ASR-P1 and Na-shlykvoite) are reproduced from the previous study [9]. Q^2 refers to a central silicon atom connected to two silicon species, e.g. silicate chains in C-S-H; Q^3 refers to a central silica atom connected to three silicon species, e.g. layered silicate sheet in clay minerals.

its morphology (see Fig. 6). The Raman spectrum of this amorphous ASR product indicates that it is similar to the synthetic ASR−P1. However, different relative intensities of the two Raman peaks at lower wavenumber range between 600 and 700 cm^{-1} are observed for this amorphous ASR product compared to the synthetic ASR−P1. For the other two amorphous ASR products formed in concrete air voids, their Raman spectra are almost identical to that of synthetic ASR-P1 as shown in Fig. 4d, except for the presence of some unknown impurities, which are most likely related to calcium carbonate [9].

Based on the coherent observations between the synthetic systems and concrete samples, recent advanced knowledge derived from synthetic systems about the structure of ASR products and their formation conditions predicted by thermodynamic modelling make it possible to get a better understanding of ASR in concrete structures. Synthetic systems showed that it was unlikely that K-shlykovite and Na-shlykovite co-precipitate in samples with mixture of KOH/NaOH as alkali source [9]. This is also the case in concrete immersed in the mixture of KOH/NaOH solution at temperature of 60 and 80 °C as confirmed in the current study. The morphological differences of ASR products formed in concrete exposed to KOH and NaOH solutions at 80 °C were also observed by others, where K-crystalline ASR product showed an elongated plate-like morphology whereas Na-crystalline ASR product was more isometric [33]. However, in most of published studies the alkali/Si ratio of ASR products was expressed as (K + Na)/Si, which did not consider

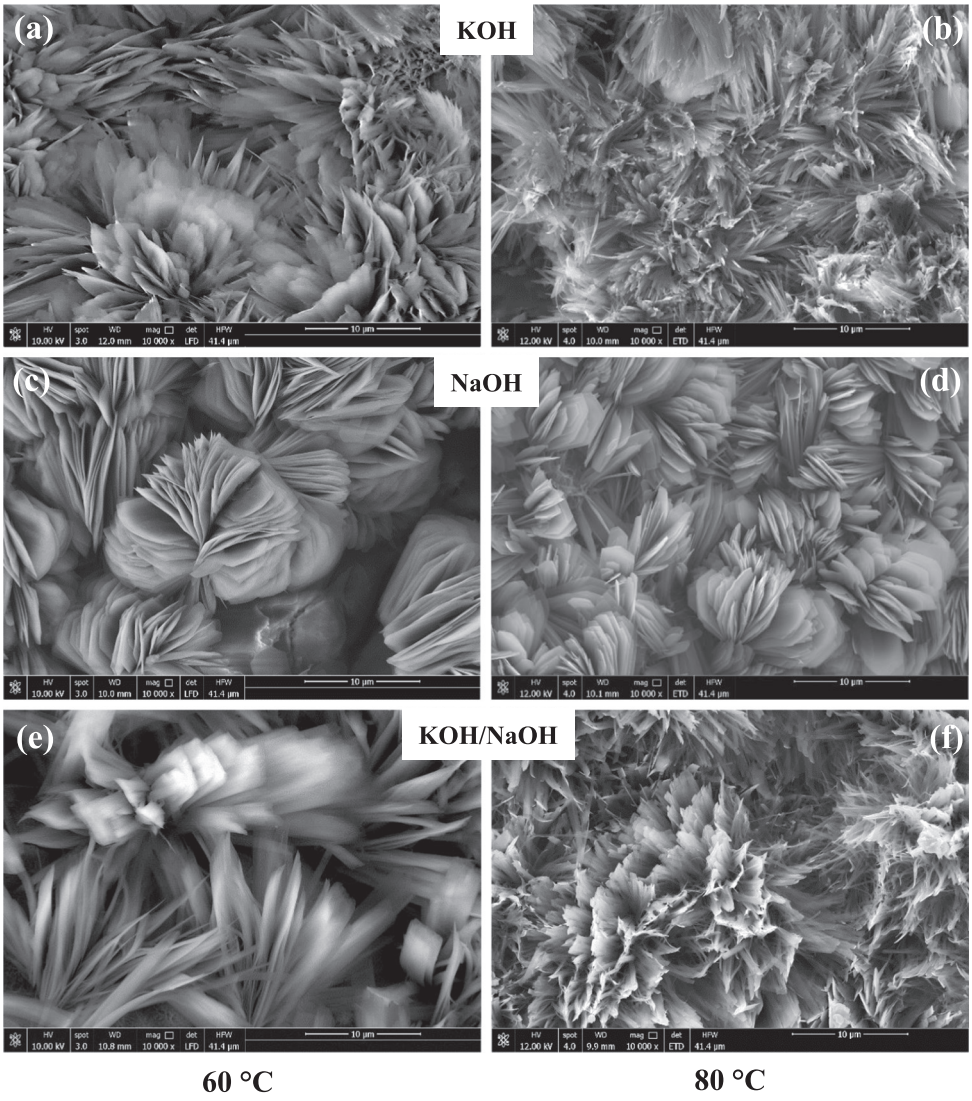

Fig. 5. Morphology of ASR products formed in the aggregates of concrete exposed to different alkaline solutions at 60 °C (left) and 80 °C (right). The image horizontal field width (HFW) is 41.4 μm for all images.

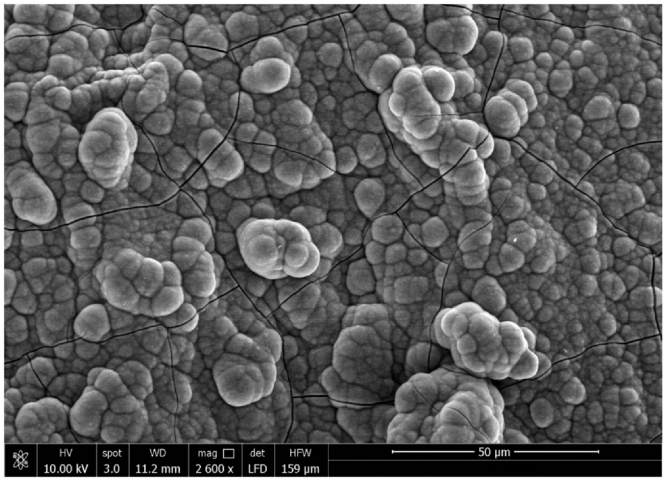

Fig. 6. Morphology of ASR-P1 within an aggregate adjacent to ITZ of concrete exposed to the mixture of KOH/NaOH solution at 60 °C.

the difference between K- and Na-ASR products.

Typical locations of ASR products in concrete are shown in Fig. 7, where crystalline ASR product is formed within the interior of aggregates and amorphous ASR products are formed within aggregates but adjacent to cement paste. Such distribution is commonly observed for most of the ASR-affected concrete [7,32]. The occurrence of crystalline ASR products in the interior of aggregates is likely attributed to the restricted availability of calcium from cement paste, whereas more calcium is available for the formation of amorphous ASR products and C-S-H close to the ITZ. Such observations match very well with the optimum conditions for ASR formation as predicted by thermodynamic modelling for synthetic systems [10]. Thermodynamic modelling also predicted that C-S-H rather than ASR products is preferably formed at very high pH due to the common ion effect [11]. This explains very well the reported lower expansion of concrete immersed in highly concentrated alkali hydroxide solution than that of concrete immersed in the corresponding alkali salt solution [5,21]. Despite that the knowledge obtained from synthetic system can explain most of the observations of ASR in concrete structures, it is important to notice that K-shlykovite, ASR-P1and Na-shlykovite are formed at 60 and 80 °C. At lower temperatures such as ≤40 °C, two other crystalline products with d-spacing of 12.0 and 10.8 Å form according to the observations from synthetic samples and field concrete [27]. The amorphous products

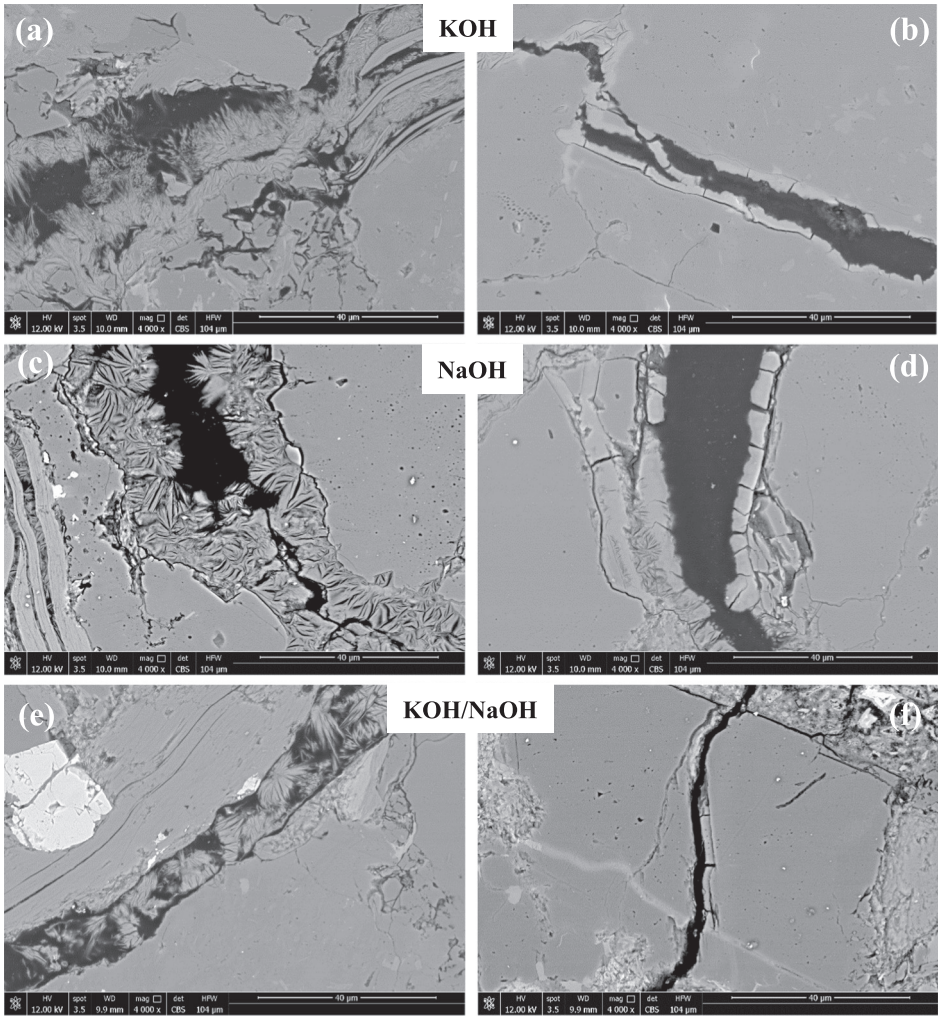

Fig. 7. SEM images on polished section containing mainly the crystalline (left) and amorphous (right) ASR products in aggregate veins of concrete exposed to sole KOH, NaOH and mixture of KOH/NaOH solution at 60 °C. The images for concrete exposed at 80 °C are similar and thus not shown here. The image horizontal field width (HFW) is 104 μm for all images.

formed at lower temperature are also different from ASR-P1 as shown in other studies, which are more similar to calcium-silicate-hydrate (C-S-H) [7,12,34]. Comparison and characterization of low temperature ASR products (both crystalline and amorphous) with different types of concrete are addressed in detail in another study [32].

4.2. Influence of alkali types on ASR expansion of concrete

Although limiting the total alkali content, which is expressed as Na_2O_{eq}, is practiced to reduce the ASR potential [35–37], Na_2O_{eq} may not always accurately define the susceptibility of cement to ASR [26]. A previous study has shown that concrete produced with cements containing a similar Na_2O_{eq} but different K/Na ratios had similar hydroxide concentration, however showed different ASR expansions [26]. The present study also shows that the types of alkalis affect the expansion of concrete as shown in Fig. 1. Similar expansion is observed between concrete prisms exposed to KOH and mixture of KOH/NaOH solutions during the entire testing period at 80 °C (Fig. 1a), and during the first 12 weeks at 60 °C (Fig. 1b). For these types of concrete, the same crystalline ASR product (K-shlykovite) is formed. Higher expansion is observed for concrete exposed to sole NaOH solution, where Na-shlykovite is formed. The results highlight the importance to distinguish the impact of different alkalis on ASR performance of concrete. Moreover, it should also be kept in mind that the role of amorphous ASR products on the expansion of concrete remains unclear. Different chemical compositions are observed for the amorphous ASR products formed in concrete exposed to KOH and mixture of KOH/NaOH solutions, with more Na-rich amorphous ASR product formed in concrete exposed to KOH/NaOH solution. However, such difference is not reflected in their ASR performance, probably due to their extremely low amounts or the Ca-containing amorphous ASR products may not contribute directly on the expansion of concrete. The impact of amorphous ASR products on ASR performance needs more investigations in future.

In any case, most of the ASR products are formed within the crack of aggregates, although some ASR products are also observed within few air voids adjacent to aggregates. This observation indicates that the ASR expansion of concrete is originated from the expansion of reactive aggregates as proposed in [13]. However, the cracks also extend into cement paste causing formation of additional C-S-H along the cracks as shown in Fig. 9. The SEM image of the post-formed C-S-H in the crack also shows several layers parallel to the crack direction as seen in Fig. 9. The EDS results show that the Ca/Si ratio of the C-S-H decreases from 1.24 to 0.93 (see Table 4) as it moves away from the cement paste (see Fig. 9), indicating that that C-S-H is accumulated perpendicular to the cracks. The formation of additional C-S-H reveals the fact that alkali–silicate solution or alkali-silicate-hydrate with low viscosity is extruded into cement paste upon initial cracking, followed by uptake of Ca from the cement paste.

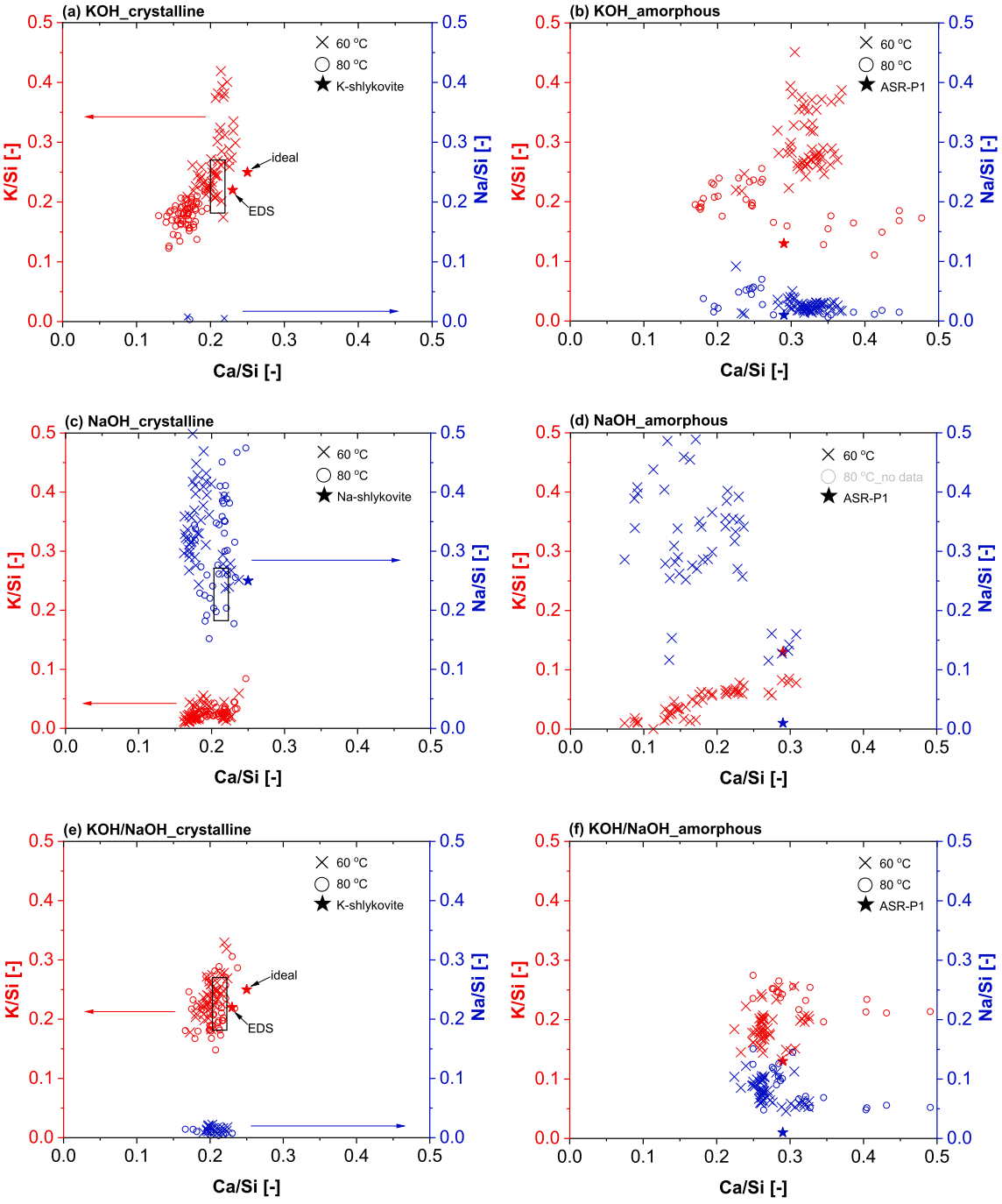

Fig. 8. Chemical compositions (atomic ratio) of ASR products formed in concrete exposed to sole KOH, NaOH and mixture of KOH/NaOH solution at 60 and 80 °C. The rectangles in the figures for the crystalline ASR products indicate the average range of chemical compositions of the crystalline ASR products formed in concrete exposed at 60 °C based the parallel study [32]. The stars indicate the chemical compositions of K-shlykovite, Na-shlykovite and ASR-P1 from the previous study [10].

4.3. Sources of ASR expansion

Several studies have shown that crystalline ASR products (Ca/Si ~ 0.25) formed at ≤80 °C and amorphous ASR product formed at 60–80 °C (e.g. ASR-P1: Ca/Si ~ 0.29) absorb only a limited amount of water, similar or even less than C-S-H [9,27,30]. A high water-uptake capacity is also not expected for Ca-rich amorphous ASR products (Ca/Si = 0.2–0.3) formed in field concrete, as they are found to be structurally similar to C-S-H [7,12]. Therefore, swelling of the Ca-rich crystalline and amorphous ASR products (Ca/Si = 0.2–0.3) is unlikely to be the main mechanism that causes expansion of concrete.

With limited availability of calcium due to spatial restrictions within aggregates, low-Ca (Ca/Si < 0.02) ASR gels are expected to form in field concrete [13,38,39]. Such ASR gels exhibit low viscosity [40,41], which leads to their extrusion into the cement paste at the point of cracking as indirectly evidenced in Fig. 9. This may partially explain the observed empty pore space left behind as shown in Fig. 9 and Fig. 6. However, cracks in field concrete are often filled with ASR products [7]. On one hand, the viscosity of the ASR gels is higher at the low temperature predominating in field concrete [42,43], such that the uptake of calcium and thus solidification of these ASR gels take place without significant extrusion. On the other hand, dissolution of silica is enhanced at higher temperature under accelerated conditions, while Ca availability remains limited, resulting in more extrusions of the low-Ca

Table 3
Average atomic ratios of the crystalline and amorphous ASR products formed in concrete exposed to sole KOH, NaOH and mixture of KOH/NaOH solutions at 60 and 80 °C. Each reported data is an average of about 50 measurements from 4 to 6 locations and about 10 measurements for each location.

	Ca/Si	K/Si	Na/Si	Ca/Si	K/Si	Na/Si
	Crystalline			Amorphous		
KOH_60 °C	0.21 ± *0.02*	0.27 ± *0.06*	–	0.32 ± *0.03*	0.30 ± *0.05*	0.03 ± *0.01*
KOH_80 °C	0.17 ± *0.01*	0.18 ± *0.02*	–	0.29 ± *0.11*	0.19 ± *0.03*	0.03 ± *0.02*
NaOH_60 °C	0.19 ± *0.02*	0.02 ± *0.01*	0.35 ± *0.08*	0.18 ± *0.06*	0.05 ± *0.02*	0.31 ± *0.10*
NaOH_80 °C	0.21 ± *0.02*	0.03 ± *0.01*	0.32 ± *0.11*	– –	– –	– –
KOH/NaOH_60 °C	0.20 ± *0.01*	0.24 ± *0.03*	0.01 *0.00*	0.27 ± *0.02*	0.19 ± *0.03*	0.08 ± *0.02*
KOH/NaOH_80 °C	0.20 ± *0.02*	0.22 ± *0.04*	0.01 *0.00*	0.32 ± *0.07*	0.23 ± *0.02*	0.09 ± *0.03*

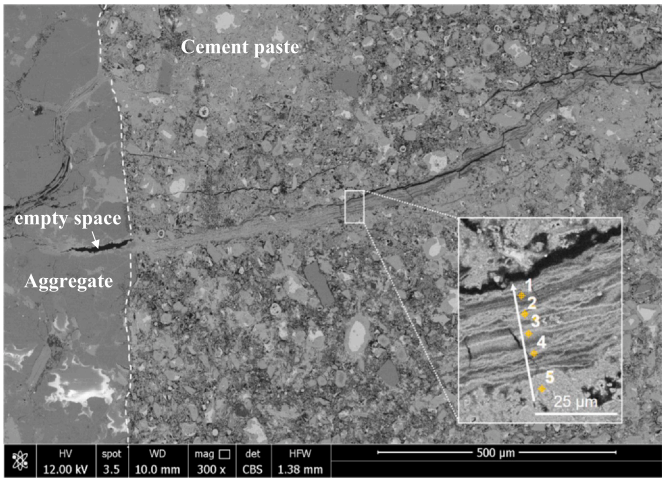

Fig. 9. C-S-H along the cracks extended into cement paste of concrete exposed to KOH solution at 60 °C. See Table 4 for the EDS analysis from location 1 to 5.

Table 4
Atomic ratios of the C-S-H present in the cracks (see Fig. 9) extended into cement paste of concrete exposed to KOH solution at 60 °C.

	Ca/Si	K/Si	Al/Si	S/Si
#1	0.93	0.14	0.06	0.00
#2	0.93	0.07	0.05	0.01
#3	0.91	0.06	0.06	0.01
#4	1.00	0.09	0.05	0.02
#5	1.24	0.08	0.08	0.02

ASR gels [42].

Based on Fig. 9, it can be deduced that there was an accumulation of low-Ca ASR gels with high flowability within the aggregate. These gels were restricted within the aggregate due to the formation of Ca-rich ASR products at aggregate/paste interface, which seems to act as a plug physically restraining an extrusion [41]. This semi-permeable plug does not restrict diffusion of concrete pore solution into the aggregate enabling further reaction [13]. As the reaction proceeds, stress is generated within the aggregate, which subsequently causes openings of the cracks and extrusion of the low-Ca ASR gels.

The formation of low-Ca ASR gels and the occurrence of their extrusion indicate their importance for the initial cracking/expansion of concrete. At later ages, the propagation of the cracks and expansion can be more complicated as crystallization of ASR products may also contribute to the crack development. Overall, the reaction kinetics, the types of alkalis, the availability of Ca, the types of ASR products and their physical and mechanical properties contribute to the damage of concrete caused by ASR.

5. Conclusions

In the current study, ASR products formed in concrete exposed to sole KOH, NaOH and mixture of KOH/NaOH solutions at high temperature (60 and 80 °C) have been characterized and compared with the ASR products synthesized at 80 °C, i.e., crystalline K- and Na-shlykovite and amorphous ASR-P1. Based on the results and discussion, the following conclusions can be drawn:

(1) The majority of ASR products are formed in the vein of aggregates, and some ASR products are formed in few air voids adjacent to the aggregates. Raman spectra and SEM/EDS results show that K-shlykovite and ASR-P1 are formed in concrete exposed to sole KOH and mixture of KOH/NaOH solutions, whereas Na-shlykovite is observed in concrete exposed to sole NaOH solution. K-shlykovite and Na-shlykovite do not co-precipitate within the same concrete, not even in those exposed to the mixture of KOH/NaOH solution.
(2) EDS results show an average Ca/Si ratio of 0.17–0.22 with little variations for all crystalline ASR products independent of exposing alkaline solutions and temperatures. In contrast, the K/Si and Na/Si ratios vary from 0.15 to 0.40. For the amorphous ASR products, both Ca/Si and alkalis/Si ratios show large variations. Both K and Na are present in the amorphous ASR products. Furthermore, a higher amount of Na is observed for the amorphous ASR products formed in concrete exposed to Na-rich alkali solution.
(3) The types of alkalis affect the expansion of concrete, where higher expansion is observed for concrete exposed to sole NaOH solution. Similar expansion is observed for concrete exposed to KOH solution and mixture of KOH/NaOH solution at the same temperature. For these two immersion conditions, the same crystalline ASR product (i.e. K-shlykovite) is formed in the concrete.
(4) The coherent observation between synthetic system and concrete prisms suggest that the information obtained for the synthetic ASR products, such as molecular structure of ASR products and the reaction conditions, can significantly improve our understandings of ASR in field concrete.

CRediT authorship contribution statement

Zhenguo Shi: Conceptualization, Methodology, Investigation, Data analysis, Writing - original draft, Writing - review & editing. **Solmoi Park:** Methodology, Investigation, Writing - review & editing. **Barbara Lothenbach:** Methodology, Investigation, Writing - review & editing. **Andreas Leemann:** Methodology, Investigation, Writing - review & editing.

Declaration of competing interest

The authors declared that they have no conflicts of interest to this work.

Acknowledgements

The authors would like to thank: a) the SNF Sinergia: alkali-silica reaction in concrete (ASR), grant number CRSII5_17108; b) the EMPAPOSTDOCS-II programme: funding from the European Union's Horizon 2020 - Research and Innovation Framework Programme under the H2020 Marie Skłodowska-Curie Actions grant agreement number 754364; and c) the Korean-Swiss Science and Technology Programme, grant number EG-KR-07-092018. Boris Ingold is acknowledged for

impregnation of the concrete samples for SEM/EDS and for some length/mass change measurements.

Data availability

The raw/processed data that support the findings of this study are available from the corresponding author upon reasonable request.

References

[1] G. West, Alkali-aggregate Reaction in Concrete Roads and Bridges, Thomas Telford, 1996.
[2] B. Fournier, M.-A. Bérubé, Alkali-aggregate reaction in concrete: a review of basic concepts and engineering implications, Can. J. Civ. Eng. 27 (2000) 167–191, https://doi.org/10.1139/l99-072.
[3] I. Sims, A.B. Poole, Alkali-aggregate Reaction in Concrete: A World Review, CRC Press, 2017, https://doi.org/10.1201/9781315708959.
[4] F. Rajabipour, E. Giannini, C. Dunant, J.H. Ideker, M.D.A. Thomas, Alkali–silica reaction: current understanding of the reaction mechanisms and the knowledge gaps, Cem. Concr. Res. 76 (2015) 130–146, https://doi.org/10.1016/j.cemconres.2015.05.024.
[5] J. Lindgård, Ö. Andiç-Çakır, I. Fernandes, T.F. Rønning, M.D.A. Thomas, Alkali–silica reactions (ASR): literature review on parameters influencing laboratory performance testing, Cem. Concr. Res. 42 (2012) 223–243, https://doi.org/10.1016/j.cemconres.2011.10.004.
[6] M. Thomas, The effect of supplementary cementing materials on alkali-silica reaction: a review, Cem. Concr. Res. 41 (2011) 1224–1231, https://doi.org/10.1016/j.cemconres.2010.11.003.
[7] A. Leemann, Raman microscopy of alkali-silica reaction (ASR) products formed in concrete, Cem. Concr. Res. 102 (2017) 41–47, https://doi.org/10.1016/j.cemconres.2017.08.014.
[8] R. Dähn, A. Arakcheeva, P. Schaub, P. Pattison, G. Chapuis, D. Grolimund, E. Wieland, A. Leemann, Application of micro X-ray diffraction to investigate the reaction products formed by the alkali–silica reaction in concrete structures, Cem. Concr. Res. 79 (2016) 49–56, https://doi.org/10.1016/j.cemconres.2015.07.012.
[9] Z. Shi, G. Geng, A. Leemann, B. Lothenbach, Synthesis, characterization, and water uptake property of alkali-silica reaction products, Cem. Concr. Res. 121 (2019) 58–71, https://doi.org/10.1016/j.cemconres.2019.04.009.
[10] Z. Shi, B. Lothenbach, The role of calcium on the formation of alkali-silica reaction products, Cem. Concr. Res. 126 (2019) 105898, , https://doi.org/10.1016/j.cemconres.2019.105898.
[11] Z. Shi, B. Lothenbach, The combined effect of potassium, sodium and calcium on the formation of alkali-silica reaction products, Cem. Concr. Res. 127 (2020) 105914, , https://doi.org/10.1016/j.cemconres.2019.105914.
[12] G. Geng, Z. Shi, A. Leemann, C. Borca, T. Huthwelker, K. Glazyrin, I.V. Pekov, S. Churakov, B. Lothenbach, R. Dähn, E. Wieland, Atomistic structure of alkali-silica reaction products refined from X-ray diffraction and micro X-ray absorption data, Cem. Concr. Res. 105958 (2020), https://doi.org/10.1016/j.cemconres.2019.105958.
[13] A. Leemann, B. Münch, The addition of caesium to concrete with alkali-silica reaction: implications on product identification and recognition of the reaction sequence, Cem. Concr. Res. 120 (2019) 27–35, https://doi.org/10.1016/j.cemconres.2019.03.016.
[14] M. Thomas, B. Fournier, K. Folliard, J. Ideker, M. Shehata, Test methods for evaluating preventive measures for controlling expansion due to alkali–silica reaction in concrete, Cem. Concr. Res. 36 (2006) 1842–1856, https://doi.org/10.1016/j.cemconres.2006.01.014.
[15] M.H. Shehata, M.D.A. Thomas, The effect of fly ash composition on the expansion of concrete due to alkali–silica reaction, Cem. Concr. Res. 30 (2000) 1063–1072, https://doi.org/10.1016/S0008-8846(00)00283-0.
[16] C.A. MacDonald, C. Rogers, R.D. Hooton, The relationship between laboratory and field expansion–observations at the Kingston outdoor exposure site for ASR after twenty years, Proc. 14th Int. Conf. Alkali-Aggregate React. Concr. (ICAAR), Austin, Texas, USA, 2012.
[17] J.H. Ideker, T. Drimalas, A.F. Bentivegna, K.J. Folliard, B. Fournier, M.D.A. Thomas, R.D. Hooton, C.A. Rogers, The importance of outdoor exposure site testing, Proc. 14th Int. Conf. Alkali Aggreg. React. ICAAR, Austin, Texas, 2014.
[18] B.C. Fournier, R. Chevrier, A. Bilodeau, P.C. Nkinamubanzi, N. Bouzoubaa, Comparative field and laboratory investigations on the use of supplementary cementing materials (SCMs) to control alkali-silica reaction (ASR) in concrete, Proc. 15th Int. Conf. Alkali Aggreg. React. (ICAAR), Sao Paolo, Bras. 2016.
[19] D.B. I., M. C., Seven years of field site tests to assess the reliability of different laboratory test methods for evaluating the alkali-reactivity potential of aggregates, Proc. 14th Int. Conf. Alkali Aggreg. React. (ICAAR), Austin, Texas, 2012.
[20] A. Leemann, C. Merz, An attempt to validate the ultra-accelerated microbar and the concrete performance test with the degree of AAR-induced damage observed in concrete structures, Cem. Concr. Res. 49 (2013) 29–37, https://doi.org/10.1016/j.cemconres.2013.03.014.
[21] S. Chatterji, N. Thaulow, A.D. Jensen, Studies of alkali-silica reaction. Part 4. Effect of different alkali salt solutions on expansion, Cem. Concr. Res. 17 (1987) 777–783, https://doi.org/10.1016/0008-8846(87)90040-8.
[22] M.-A. Bérubé, J. Duchesne, J.F. Dorion, M. Rivest, Laboratory assessment of alkali contribution by aggregates to concrete and application to concrete structures affected by alkali–silica reactivity, Cem. Concr. Res. 32 (2002) 1215–1227, https://doi.org/10.1016/S0008-8846(02)00766-4.
[23] J. Lindgård, M.D.A. Thomas, E.J. Sellevold, B. Pedersen, Ö. Andiç-Çakır, H. Justnes, T.F. Rønning, Alkali–silica reaction (ASR)—performance testing: influence of specimen pre-treatment, exposure conditions and prism size on alkali leaching and prism expansion, Cem. Concr. Res. 53 (2013) 68–90, https://doi.org/10.1016/j.cemconres.2013.05.017.
[24] X. Li, D. Gress, Mitigating alkali-silica reaction in concrete containing recycled concrete aggregate, Transp. Res. Rec. J. Transp. Res. Board. 1979 (2006) 30–35, https://doi.org/10.3141/1979-06.
[25] A. Shayan, H. Morris, A comparison of RTA T363 and ASTM C1260 accelerated mortar bar test methods for detecting reactive aggregates, Cem. Concr. Res. 31 (2001) 655–663, https://doi.org/10.1016/S0008-8846(00)00491-9.
[26] A. Leemann, B. Lothenbach, The influence of potassium–sodium ratio in cement on concrete expansion due to alkali-aggregate reaction, Cem. Concr. Res. 38 (2008) 1162–1168, https://doi.org/10.1016/j.cemconres.2008.05.004.
[27] Z. Shi, A. Leemann, D. Rentsch, B. Lothenbach, Synthesis of alkali-silica reaction product structurally identical to that formed in field concrete, Mater. Des. 190 (2020) 108562, , https://doi.org/10.1016/j.matdes.2020.108562.
[28] N.V. Zubkova, Y.E. Filinchuk, I.V. Pekov, D.Y. Pushcharovsky, E.R. Gobechiya, Crystal structures of shlykovite and cryptophyllite: comparative crystal chemistry of phyllosilicate minerals of the mountainite family, Eur. J. Mineral. 22 (2010) 547–555, https://doi.org/10.1127/0935-1221/2010/0022-2041.
[29] A. Leemann, I. Borchers, M. Shakoorioskooie, M. Griffa, C. Müller, P. Lura, Microstructural analysis of ASR in concrete - accelerated testing versus natural exposure, Proc. Pro128 Int. Conf. Sustain. Mater. Syst. Struct. (SMSS2019). Durability, Monit. Repair Struct. RILEM Publ. S.A.R.L, Paris, Fr. Rilem Publications, Paris, 2019.
[30] A. Leemann, Z. Shi, M. Wyrzykowski, F. Winnefeld, Moisture stability of crystalline alkali-silica reaction products formed in concrete exposed to natural environment, Mater. Des. 195 (2020) 109066.
[31] C.M. Strack, E. Barnes, M.A. Ramsey, R.K. Williams, K.L. Klaus, R.D. Moser, Impact of aggregate mineralogy and exposure solution on alkali-silica reaction product composition and structure within accelerated test conditions, Constr. Build. Mater. 240 (2020) 117929, , https://doi.org/10.1016/j.conbuildmat.2019.117929.
[32] A. Leemann, Z. Shi, J. Lindgård, Characterization of amorphous and crystalline ASR products formed in concrete aggregates, Cem. Concr. Res. 137 (2020) 106190.
[33] G. Davies, R.E. Oberholster, Alkali-silica reaction products and their development, Cem. Concr. Res. 18 (1988) 621–635, https://doi.org/10.1016/0008-8846(88)90055-5.
[34] C. Balachandran, J.F. Muñoz, T. Arnold, Characterization of alkali silica reaction gels using Raman spectroscopy, Cem. Concr. Res. 92 (2017) 66–74, https://doi.org/10.1016/j.cemconres.2016.11.018.
[35] M.L. Leming, B.Q. Nguyen, Limits on alkali content in cement—results from a field study, Cem. Concr. Aggregates. 22 (2000) 41–47, https://doi.org/10.1520/CCA10462J.
[36] E.D. Hill, Alkali limits for prevention of alkali-silica reaction: a brief review of their development, Cem. Concr. Aggregates. 18 (1996) 3–7, https://doi.org/10.1520/CCA10305J.
[37] K. Tosun, B. Felekoğlu, B. Baradan, The effect of cement alkali content on ASR susceptibility of mortars incorporating admixtures, Build. Environ. 42 (2007) 3444–3453, https://doi.org/10.1016/j.buildenv.2006.08.024.
[38] C.E. Tambelli, J.F. Schneider, N.P. Hasparyk, P.J.M. Monteiro, Study of the structure of alkali–silica reaction gel by high-resolution NMR spectroscopy, J. Non-Cryst. Solids 352 (2006) 3429–3436, https://doi.org/10.1016/j.jnoncrysol.2006.03.112.
[39] T. Katayama, ASR gels and their crystalline phases in concrete—universal products in alkali–silica, alkali–silicate and alkali–carbonate reactions, Proc. 14th Int. Conf. Alkali Aggreg. React. (ICAAR), Austin, Texas, 2012, pp. 20–25.
[40] L.J. Struble, S. Diamond, Swelling properties of synthetic alkali silica gels, J. Am. Ceram. Soc. 64 (1981) 652–655, https://doi.org/10.1111/j.1151-2916.1981.tb15864.x.
[41] R.F. Bleszynski, M.D.A. Thomas, Microstructural studies of alkali-silica reaction in fly ash concrete immersed in alkaline solutions, Adv. Cem. Based Mater. 7 (1998) 66–78, https://doi.org/10.1016/S1065-7355(97)00030-8.
[42] Y. Kawabata, C. Dunant, K. Yamada, K. Scrivener, Impact of temperature on expansive behavior of concrete with a highly reactive andesite due to the alkali–silica reaction, Cem. Concr. Res. 125 (2019) 105888, , https://doi.org/10.1016/j.cemconres.2019.105888.
[43] A.G. Vayghan, F. Rajabipour, J.L. Rosenberger, Composition–rheology relationships in alkali–silica reaction gels and the impact on the gel's deleterious behavior, Cem. Concr. Res. 83 (2016) 45–56, https://doi.org/10.1016/j.cemconres.2016.01.011.